

Specific heat of $\text{Ni}(\text{NO}_3)_2 \cdot 6\text{NH}_3$ between 0.4 and 20 K*

W. Sano and S. R. Salinas

Instituto de Física, Universidade de São Paulo, C.P. 20516-São Paulo, Brasil

(Received 8 September 1976)

The specific heat of $\text{Ni}(\text{NO}_3)_2 \cdot 6\text{NH}_3$ has been measured between 0.4 and 20 K in a mechanical heat switch calorimeter. A sharp λ -like anomaly occurs at the Néel temperature $T_N = 1.345$ K. The experimental entropy of the transition was determined to be $\Delta S = 9.125$ J/K mol, in quite good agreement with the theoretical value $R \ln(2S + 1) = 9.137$ J/K mol for $S = 1$. Since EPR measurements indicate that the anisotropy in these crystals is not large, a Heisenberg three-dimensional Hamiltonian has been used for modeling the magnetic behavior. The mean-field approximation indicates that the antiferromagnetic ordering is of the second kind in an fcc lattice. A best fit of the experimental data to a high-temperature expansion yields values for the exchange parameters $J_1 = -0.125$ K and $J_2 = -0.38$ K which are consistent with this kind of order.

INTRODUCTION

Hexammine nickel nitrate, $\text{Ni}(\text{NO}_3)_2 \cdot 6\text{NH}_3$, which we shall hereafter refer to as NNA, forms face-centered-cubic crystals with lattice parameter $a = 10.98$ Å.¹ The nickel ions occupy the sites of the fcc lattice, while the six ammonia molecules form a regular octahedron centered at each site. The NO_3 groups surround these octahedrons and are disposed in a cubic lattice of edge $\frac{1}{2}a$. The $m\bar{3}(T_h)$ symmetry attributed to this crystal by Wyckoff was later contested by Kracek and collaborators² who concluded that the NO_3 groups rotate inside the unit cell. Yu³ performed more complete measurements using x rays between 80 and 300 K. He concluded that the triangular-shaped NO_3 groups are oscillating with large amplitudes about one of their edges, and that $m\bar{3}m(O_h)$ is the most probable symmetry group for this crystal.

The thermal properties of NNA were initially studied through differential-thermal-analysis measurements performed by Jensen and Beevers.⁴ They suggested the existence of a λ -type transition at -28.6 °C. Later, Long and Toettcher⁵ measured the specific heat between 54 and 300 K in order to confirm this prediction. A λ -type anomaly is apparent at 243.3 K and was attributed⁵ to an order-disorder transition of the nitrate and ammonia molecules. They also reported a small specific-heat anomaly below 80 K. Recently, Bousquet and collaborators⁶ studied this anomaly with specific-heat experiments between 9 and 300 K and concluded that it always depends on the thermal history of the sample. Considerable efforts were spent to explain the high-temperature λ -type transition. There are several investigations using dilatometric techniques,⁷ ultrasonic techniques,⁸ infrared,⁹ and EPR.¹⁰ At present we think that the nature of this phenomenon is analogous to the cooperative transition of the ammonia observed

in other well-known isomorphous metal hexamine complexes.

The magnetic properties of NNA were first studied in our laboratory by magnetic-susceptibility and specific-heat measurements performed at liquid-helium temperatures. A new λ -type peak was observed in the specific-heat measurements at about 1.35 K, where the susceptibility data indicate a corresponding anomaly due to a paramagnetic to an antiferromagnetic transition.¹¹ A H -vs- T phase diagram from susceptibility measurements in applied magnetic fields up to 70 kOe confirmed this assumption.¹² So we decided to build a mechanical heat-switch calorimeter and to undertake more-detailed measurements of the specific heat of NNA between 0.4 and 20 K. It is the purpose of our paper to present the results of this investigation.

SAMPLE PREPARATION AND APPARATUS

$\text{Ni}(\text{NO}_3)_2 \cdot 6\text{NH}_3$ samples have been obtained by reacting NiCO_3 (Baker Analyzed Reagent) with HNO_3 (Reagent PA) and adding NH_4OH (Berzog PA) in excess to the solution. Small octahedral blue crystals of approximately 2 mm along the largest dimension were obtained in the solution and were recrystallized once more before separating and drying. They were dried in a desiccator over silica gel in an atmosphere of ammonia to prevent decomposition by ammonia loss. Ammonia analysis by a distillation process in a micro-Kjeldahl apparatus indicated the presence of six ammonia molecules per nickel, within 99.5% of precision.

Samples of about 10 g were encapsulated in a copper box for performing the specific-heat measurements. The box surface was covered with a thin covering of gold to prevent any chemical reactions due to the presence of ammonia in the sample. A carbon thermometer and heater (a

Mial metalized resistor) were attached to the sample box. The heat capacity of the box and its addenda were determined in a separate series of experiments. The correction for this contribution was less than 8% at 4 K.

The sample box was held by a nylon thread inside a vacuum chamber, beneath the liquid- ^3He reservoir. A hinged lever, which acts as a heat switch, was attached to the bottom of the reservoir, in good thermal contact with it. This lever could be commanded by a thin stainless steel wire connected to the top of the cryostat. The lever presses the sample capsule lid to cool it through thermal contact with the ^3He bath. There is also a spring to ensure the opening of the heat switch when one needs to break the thermal contact.

Between 0.4 and 4 K we used a Speer carbon thermometer (470Ω , $\frac{1}{2} \text{ W}$) for our calorimetric measurements. The calibration of this thermometer was achieved with ^4He vapor-pressure measurements (1.2–4.2 K) and the use of a magnetic cerium-magnesium-nitrate thermometer (below 1.2 K) in each experiment. The cerium-magnesium-nitrate salt was attached to the liquid- ^3He reservoir and the calibration was processed after closing the mechanical heat switch. The Speer thermometer was well described by the Balcombe *et al.*¹³ equation

$$T = C_1 / (\ln R - C_2)^{C_3},$$

where C_1 , C_2 , and C_3 are adjustable constants; T is the absolute temperature, and R is the electrical resistance. Between 4 and 20 K we used an Allen Bradley carbon resistor (270Ω , $\frac{1}{8} \text{ W}$). Between 4 and 14 K this resistor was calibrated by a magnetic manganous-ammonium-sulfate (MAS) thermometer and a Ge thermometer which were previously calibrated in liquid hydrogen between 14 and 20 K.

Our R -vs- T points were well described by the Clement-Quinnell¹⁴ law

$$T = a / (\ln R + b / \ln R - c),$$

where a , b , and c are adjustable parameters. All the adjustable parameters were determined in a best fitting computer calculation using all the experimental data. Additional details of the apparatus and the experimental procedures were described elsewhere.¹⁵

RESULTS AND DISCUSSION

The heat capacity C_p of NNA was determined experimentally between 0.4 and 20 K. The results near the transition point are shown in Fig. 1. All the experimental specific-heat data presented in Fig. 1 and in other figures are representative of a large number of experiments on several inde-

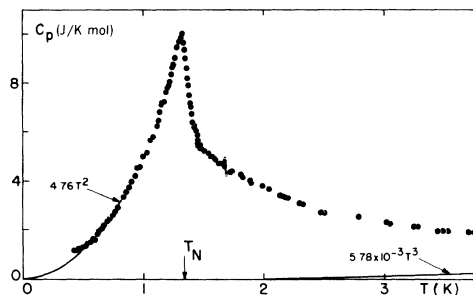


FIG. 1. Specific heat vs temperature in the paramagnetic-to-antiferromagnetic transition region. The $4.76T^2$ law shown at the low-temperature side is the extrapolation of the magnetic contribution. The $5.78 \times 10^{-3} T^3$ law at the high-temperature side is the lattice contribution.

pendently prepared specimens. The sharp λ -type peak characteristic of a paramagnetic to anti-ferromagnetic transition establishes the Néel temperature as $T_N = 1.345 \pm 0.005 \text{ K}$. The specific heat at this temperature is $10.02 \pm 0.05 \text{ J/K mol}$. These values are average results over several runs, and the associated uncertainties reflect differences among these runs. A Néel point of this magnitude is consistent with previous results from magnetic susceptibility measurements.¹¹ The value of dX/dT near T_N shows an anomaly at the same Néel temperature indicated by the specific-heat experiments.

Now we wish to describe a more complete investigation of the specific-heat behavior. For this purpose we measured again the specific heat between 0.4 and 3.0 K and obtained new data up to 20 K.

At low temperatures earlier experiments indicated the beginning of an increase of the specific-heat values for decreasing temperatures below 0.4 K. This is also consistent with our new data. Since the susceptibility measurements rule out any contribution from new magnetic degrees of freedom to this anomalous behavior, we are led to attribute it to the tunneling of the ammonia molecules, similarly to what has been observed by Van Kempen and others¹⁶ in isomorphous nickel hexamine halogenides. From 0.5 to 0.9 K we were able to fit the experimental specific heat data to the power law $C_p = 4.76T^2$. This fitting which takes into account the magnetic contribution for $T \ll T_N$ is shown in Fig. 1. The points which were not fitted at the low-temperature end of the curve are related to the tunneling effect of the ammonia molecules.

In the transition region the lattice contribution is small, as plotted in Fig. 1, becoming important only at high temperatures. For $T \gg T_N$ it is possible to describe the specific heat by the equation

$$C_p = aT^3 + bT^{-2},$$

where the first term represents the contribution of the lattice vibrations to the heat capacity (Debye's law) and the second term is the high-temperature magnetic contribution. In this last term we consider the Schottky contribution, due to the splitting of the spin levels brought about by the distortion of the cubic crystal-field symmetry, and the dominating high-temperature term due to short-range spin-spin interactions. A best fitting of the data yields the values

$$a = 5.78 \times 10^{-3} \text{ J/K}^4 \text{ mol}, \quad b = 24 \text{ J K/mol}.$$

This law is well observed between 5 and 10 K, as it is indicated by a plot of $C_p T^2$ vs T^5 shown in Fig. 2. The angular coefficient of this straight line gives the value of a , while b is given by the linear intercept.

The experimental C_p data at the high-temperature side are shown in Fig. 3.

It is well known that specific-heat data provide valuable information about short-range magnetic interactions. So we should be able to analyze our measurements and to extract additional details beyond the simple term b/T^2 . However, we have initially to consider the magnitude of the Schottky effect produced by the distortion of the crystal-field symmetry.

Infrared⁹ and EPR¹⁰ measurements made by our group indicated that the crystal field at the Ni^{++} ion is cubic with trigonal distortion. This distortion is a consequence of the arrangement of the NH_3 molecules in the crystal. It splits the $S = 1$ spin state of nickel into a doublet and a singlet with an energy difference $D = 0.841$ K. We obtained this value through EPR measurements performed at liquid-nitrogen temperatures and assumed that it remains practically unchanged at lower temperatures. This is a small value compared with the

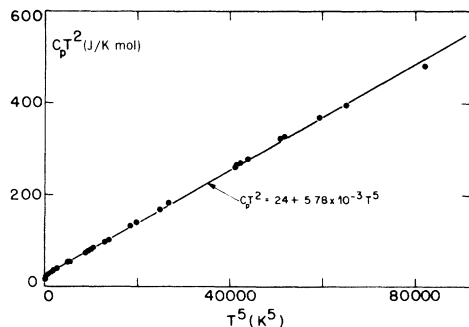


FIG. 2. $C_p T^2$ -vs- T^5 plot showing the straight line $C_p T^2 = 24 + 5.78 \times 10^{-3} T^5$. The linear coefficient is the value corresponding to the magnetic contribution for $T \gg T_N$, and the angular coefficient is the value corresponding to the Debye T^3 law.

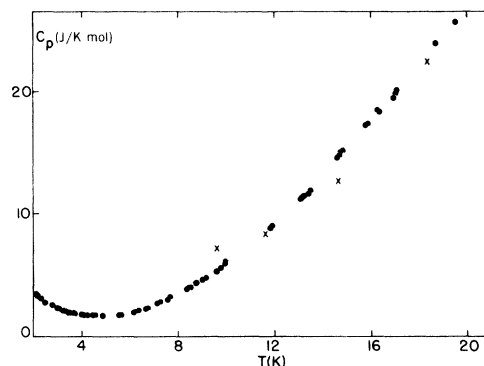


FIG. 3. Experimental specific heat vs temperature above the transition. The full dots are our measurements and the crosses are from Ref. 6.

Weiss temperature $\Theta = -3.3$ K obtained from the susceptibility measurements,¹¹ and makes it possible to consider NNA as a crystal of small anisotropy. This small anisotropy and the fcc structure of NNA support the three-dimensional Heisenberg Hamiltonian as a good approximation for modeling the antiferromagnetic interactions.

In fcc crystals a given ion has 12 first neighbors, and one of these has always two neighbors among the same set of 12 ions. It is geometrically impossible to produce an antiparallel order of all these 12 ions. So it is necessary to consider interactions between first and between second neighbors to understand the antiferromagnetic order, no matter the magnitude of the second-neighbor interaction. As a consequence, we need to take into account more than two sublattices. The inclusion of the second neighbors makes the solution of the Hamiltonian considerably more laborious. The inclusion in the Hamiltonian of the anisotropy term DS_z^2 leads to additional complications. However, this last trouble is not important if the value of D is small. In this case we can subtract the Schottky contribution from the specific heat and assume that the remaining magnetic interactions are essentially described by the Heisenberg Hamiltonian

$$H = -2J_1 \sum_{(i,j)} \tilde{S}_i \cdot \tilde{S}_j - 2J_2 \sum_{(k,l)} \tilde{S}_k \cdot \tilde{S}_l,$$

where the first sum is over pairs of nearest neighbors, and the second sum over pairs of next-nearest neighbors.

This Hamiltonian is usually studied within the framework of the mean-field approximation. Smart¹⁷ divides the fcc lattice into eight sublattices and uses the mean-field approximation to identify three kinds of antiferromagnetically ordered ground states (AF1, AF2, and AF3), corresponding to particular patterns of spin arrange-

ments. The existence of these arrangements was confirmed experimentally by neutron diffraction techniques in fcc crystals like MnO, FeO, CoO, NiO, and α -MnS.¹⁷ This encouraged us to use the same mean-field results to interpret our specific-heat data.

The specific-heat data can be integrated to yield an experimental value for the magnetic energy of the ground state. This value has to be compared with the mean field predictions for the three distinct types of spin arrangements. The magnetic ground-state energy is

$$E_0 = \int_0^\infty C_m(T) dT,$$

where $C_m(T)$ is the experimental magnetic specific heat. Between 0.8 and 3.5 K we performed a simple numerical integration. At low temperatures (from 0 to 0.8 K) we used the extrapolation law $4.76T^2$ for the magnetic specific heat. At high temperatures (3.5 K to ∞) we used the high-temperature expansion of the magnetic specific heat. This procedure yields the value $E_0 \approx 18$ J, to be compared with the classical approximation for the three types of orderings predicted by the mean-field approximation.

The value of Θ/T_N gives an initial indication about the type of ground-state arrangement to be chosen. For NNA it is approximately -2.5 , being consistent with the AF1 and the AF2 types of antiferromagnetism. We decided which order is most favorable by taking into account the value of the ground-state energy.

For the AF1 kind of order, Smart's results indicate $J_1 \gg J_2$, such that we can consider only first-neighbor interactions for the theoretical determination of E_0 . The energy of the eight antiparallel and the four parallel first neighbors of the AF1 kind of order gives $E_0 = -4R(J_1/k)S^2$. From this expression we obtain $J_1 = -0.54$ K. However, this value is not in agreement with the value $J_1 = -0.21$ K obtained from the expression for the Weiss temperature

$$\Theta = 2zJ_1S(S+1)/3k,$$

where Θ comes from the magnetic susceptibility measurements. This disagreement is an indication that AF1 is not the kind of order suitable for NNA.

In the AF2 type of order, each ion has six parallel first neighbors and six antiparallel first neighbors. So the energy comes entirely from the interactions between the six antiparallel second neighbors, that is,

$$E_0 = -6R(J_2/k)S^2$$

from which we have $J_2 = -0.36$ K. For this type of order the Weiss temperature is given by

$$\Theta = [2S(S+1)/3K](12J_1 + 6J_2).$$

Now Θ depends on J_1 and J_2 , and the experimental value, given by the magnetic susceptibility measurements, is not enough for checking the values of the exchange parameters. Instead of using the mean-field expression of Θ for testing this type of spin arrangement, we turned our attention to the high-temperature specific-heat data. The best fitting of the specific data to the high-temperature expansion yields $J_1 = -(0.125 \pm 0.002)$ K and $J_2 = -(0.38 \pm 0.02)$ K. Despite neglecting the effects of zero-point spin-wave motions, the predictions from the mean-field expression of the ground-state energy agree very nicely with this latter value of J_2 . Also, the ratio J_2/J_1 obtained from the values produced by the high-temperature fitting to the specific-heat data is consistent with the AF2 type of order. So we suggest that the spins in NNA order according to the AF2 type of antiferromagnetic arrangement.

Now we wish to make some comments about our best fitting of the specific-heat data with the high-temperature expansion. Dalton calculated several terms of an expansion for the free energy of Ising and Heisenberg ferromagnetic models using first- and second-neighbor interactions, for several spin values, in different kinds of lattices.¹⁸ At the present day his work contains the longest available expansions for model Hamiltonians with first- and second-neighbor interactions. Using these results we derived an expression for the specific heat in our particular case: an antiferromagnetic Heisenberg model, with $S=1$, in an fcc lattice. The specific heat per spin is

$$C_m = \sum_{r+s=2}^6 C_{rs} \left(\frac{J_1}{kT}\right)^r \left(\frac{J_2}{kT}\right)^s,$$

where the coefficients C_{rs} are $C_{20}=32$, $C_{02}=16$, $C_{30}=309.3333$, $C_{21}=512$, $C_{12}=0$, $C_{03}=-16$, $C_{40}=2346.6666$, $C_{31}=7850.6666$, $C_{22}=2901.333$, $C_{13}=0$, $C_{04}=64$, $C_{50}=19757.0370$, $C_{41}=79075.5555$, C_{32}

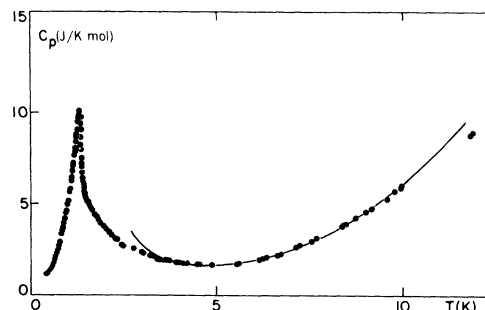


FIG. 4. Specific heat vs temperature. The dots are experimental values and the curve comes from the theoretical model.

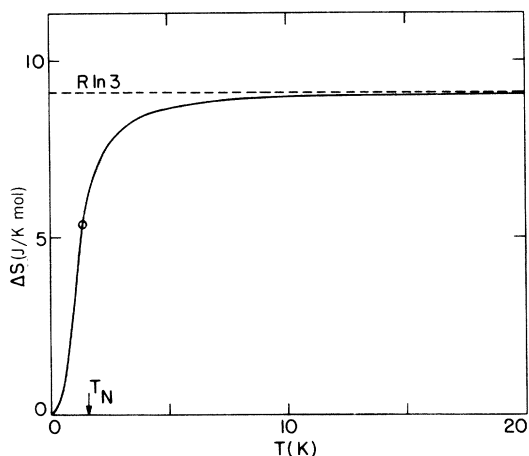


FIG. 5. Entropy of magnetic transition versus temperature. The curve is the experimental value. The circle on this curve indicates the Néel point. The dashed line indicates $R \ln 3$, which is the theoretical value of the entropy at $T = \infty$.

= 96 426.6666, $C_{23} = 40\,296.2963$, $C_{14} = 0$, $C_{05} = 65.185\,185$, $C_{60} = 183\,474.5479$, $C_{51} = 813\,928.2960$, $C_{42} = 1\,530\,604.8110$, $C_{33} = 948\,603.2592$, $C_{24} = -24\,319.9999$, $C_{15} = 0$, and $C_{06} = -6847.9991$. Adjusting this series to our experimental data for the specific heat we obtain the parameters J_1 and J_2 . In Fig. 4 we show a theoretical curve for the specific heat, including the contributions from the series expansions, the Schottky anomaly, and the lattice vibrations. The fitting is very good down to 3.5 K. Below 3.5 K the theoretical expression begins to deviate from the experimental data. New terms of the high-temperature expansion must probably be included or maybe the three-dimensional Heisenberg model is not really adequate

close to the critical point. It is important to remark that since D is small we are treating the Schottky term and the Heisenberg Hamiltonian separately. This approximation makes it possible to perform series analysis of the Heisenberg model with first- and second-nearest-neighbor interactions. However, the agreement at high temperatures, when the truncated series should work best, is really very good.

Below T_N the dependence of the specific heat on T^2 is an unexpected fact. Kubo¹⁹ obtained a T^2 law for the specific heat of a two-dimensional model using spin-wave theory. Three-dimensional crystals with no anisotropy exhibit a T^3 law. Our experimental data are not sufficient to give an ultimate conclusion about the T^2 variation and we did not make any study to verify the possibility of a two-dimensional behavior.

An important test of our conclusions is the comparison between the experimental and the theoretical values of the entropy change through the transition. The total theoretical entropy of transition is given by $\Delta S = R \ln(2S + 1)$, where S is the spin value. In Fig. 5 we show the experimental graph of ΔS vs T . Most of the entropy is between 0.4 and 3.5 K, where this graph was obtained through a numerical integration. The extrapolated value below 0.4 K amounted to about 10% of the total entropy. Above 3.5 K it was possible to use the high-temperature series for a more-reliable extrapolation (about 5% of the total value). It is possible to observe that the experimental ΔS curve tends smoothly to the theoretical value $\Delta S = R \ln 3 = 9.137$ J/K mol. The total experimental entropy is $\Delta S = 9.125 \pm 0.015$ J/K mol, about 0.13% below the theoretical value. This close agreement lends additional support to the assumptions of our work.

*Supported by Financiadora de Estudos e Projetos and Conselho Nacional de Desenvolvimento Científico e Tecnológico.

¹R. W. G. Wyckoff, *J. Am. Chem. Soc.* **44**, 1260 (1922).

²F. C. Kracek, S. B. Hendricks, and E. Posujak, *Nature* **128**, 410 (1931).

³S. H. Yu, *Nature* **141**, 158 (1938).

⁴A. T. Jensen and C. A. Beevers, *Trans. Faraday Soc.* **34**, 1478 (1938).

⁵E. A. Long and F. C. Toettcher, *J. Chem. Phys.* **8**, 504 (1940).

⁶J. Bousquet, M. Prost, and M. Diot, *J. Chim. Phys. (France)* **6**, 1004 (1972).

⁷D. G. Thomas, L. A. K. Staveley, and A. F. Cullis, *J. Chem. Soc.* 1727 (1952).

⁸S. Haussuhl, *Acta Crystallogr. A* **30**, 455 (1974).

⁹S. Isotani, W. Sano, and J. A. Ochi, *J. Phys. Chem. Solids* **36**, 95 (1975).

¹⁰J. A. Ochi, W. Sano, S. Isotani, and C. E. Hennies, *J. Chem. Phys.* **62**, 2115 (1975).

¹¹C. C. Becerra, W. Sano, A. Marques, G. Frossatti, A. Paduan, Jr., N. F. Oliveira, Jr., and C. J. A. Quadros, *Phys. Lett. A* **40**, 203 (1972).

¹²A. Paduan, Jr. and N. F. Oliveira, Jr., *Phys. Lett. A* **46**, 117 (1973).

¹³R. J. Balcombe, D. J. Emerson, and R. J. Potton, *J. Phys. E* **3**, 43 (1970).

¹⁴J. R. Clement and E. H. Quinell, *Rev. Sci. Instrum.* **23**, 213 (1952).

¹⁵W. Sano, Doctoral thesis (University of São Paulo, 1975) (unpublished).

¹⁶H. van Kempen, W. T. Duffy, Jr., A. R. Miedema, and W. J. Huiskamp, *Physica (Utr.)* **30**, 1131 (1964); and H. van Kempen, T. Garofano, A. R. Miedema, and W. J. Huiskamp, *ibid.* **31**, 1096 (1965).

¹⁷J. S. Smart, *Effective Field Theories of Magnetism* (Saunders, Philadelphia, 1966), Chap. 8.

¹⁸N. W. Dalton, *Proc. Phys. Soc. Lond.* **88**, 659 (1966).

¹⁹R. Kubo, *Phys. Rev.* **87**, 568 (1952).